

# Molecular Modeling Studies on Oxidation of Hexopyranoses by Galactose Oxidase. An Active Site Topology Apparently Designed To Catalyze Radical Reactions, Either Concerted or Stepwise

Rebekka M. Wachter and Bruce P. Branchaud\*

Contribution from the Department of Chemistry and the Institute of Molecular Biology, University of Oregon, Eugene, Oregon 97403

Received June 19, 1995<sup>⊗</sup>

**Abstract:** Galactose oxidase is a mononuclear copper enzyme which oxidizes primary alcohols to aldehydes using molecular oxygen. A unique type of cross-link between tyrosine 272, an active site copper ligand, and cysteine 228 provides a modified tyrosine radical site which is believed to act as a one-electron redox center. Galactose oxidase is highly selective in its processing of hexopyranose substrates. Turnover of D-galactose is stereospecific for cleavage of the *pro-S* hydrogen. D-Galactose is an excellent substrate but its C-4 epimer D-glucose is not a substrate and will not even bind at 1 M concentration. Any proposed mechanism for galactose oxidase should be able to account for these stringent hexopyranose substrate specificities. In this paper we report molecular modeling studies of active site binding of postulated radical carbon–hydrogen bond cleavage transition states of D-galactose and D-glucose. Differences in specific enzyme–substrate interactions provide convincing explanations of the *pro-S* and galactose specificities. In addition, a previously unconsidered concerted radical mechanism appears to be just as plausible as the more standard stepwise radical mechanism via a ketyl radical anion intermediate. Regardless of whether a stepwise or concerted mechanism is operating, the active site appears to be well designed to bind radical transition states and perform radical enzyme catalysis. The detailed models developed here for ground state and transition state enzyme–substrate interactions provide insight to guide mechanistic studies using both radical-probing substrates and site-directed mutagenesis.

In recent years evidence has been accumulating that many enzymes proceed through radical mechanisms.<sup>1</sup> Most of these reactions involve redox cofactors for which radical intermediates are quite plausible based on model studies of cofactor chemistry. New types of mechanisms have been proposed recently involving protein radicals, mostly on amino acid side chains,<sup>2</sup> but even on the protein backbone as in pyruvate formate lyase.<sup>3</sup> H-atom abstraction from a substrate by a protein-derived radical is likely to occur in the mechanisms of several of these protein radical enzymes including the various types of ribonucleotide reductases (binuclear iron + tyrosyl radical, adenosylcobalamin [B<sub>12</sub>] + protein radical, binuclear manganese + protein radical),<sup>4</sup> several B<sub>12</sub> enzymes,<sup>5</sup> and prostaglandin H-synthase (mononuclear iron + tyrosyl radical) in prostaglandin biosynthesis.<sup>6</sup>

Galactose oxidase (GOase) from the filamentous wheat-rot fungus *Fusarium spp.*<sup>7</sup> catalyzes the oxidation of primary alcohols with O<sub>2</sub>, producing aldehydes and H<sub>2</sub>O<sub>2</sub> (RCH<sub>2</sub>OH + O<sub>2</sub> = RCHO + H<sub>2</sub>O<sub>2</sub>).<sup>8</sup> It is a single polypeptide with a molecular mass of 68 500. For many years a single copper was the only known redox center in GOase. This caused problems in the formulation of mechanisms for two-electron catalysis for an enzyme which had been believed to possess a single copper one-electron redox center. One proposed mechanism involved a shuttling between Cu(III) and Cu(I) oxidation states.<sup>9</sup> Another proposed mechanism used a shuttling between Cu(II) and Cu(I) oxidation states for sequential one-electron transfers to O<sub>2</sub>.<sup>10</sup> For a brief time it was believed that GOase might contain pyrroloquinoline quinone (PQQ) as a redox cofactor.<sup>11</sup> Spectroscopic evidence and, especially, high-resolution X-ray crys-

<sup>⊗</sup> Abstract published in *Advance ACS Abstracts*, March 1, 1996.

(1) (a) Frey, P. A. *Chem. Rev.* **1990**, *90*, 1343–57. (b) Baldwin, J. E.; Bradley, M. *Chem. Rev.* **1990**, *90*, 1079–88. (c) Stubbe, J. *Biochemistry* **1988**, *27*, 3893–3900. (d) Booker, S.; Broderick, J.; Stubbe, J. *Biochem. Soc. Trans.* **1993**, *21*, 727–730. (e) Pederson, J. Z.; Finazzi-Agrò, A. *FEBS* **1993**, *325*, 53–58.

(2) (a) Stubbe, J. *Annu. Rev. Biochem.* **1989**, *58*, 257–285. (b) Prince, R. C. *Trends Biochem. Sci.* **1988**, *13*, 286–288. (c) Tsai, A.-L.; Palmer, G.; Kulmacz, R. J. *J. Biol. Chem.* **1992**, *267*, 17753–17759. (d) DeGray, J. A.; Lassmann, G.; Curtis, J. F.; Kennedy, T. A.; Marnett, L. J.; Eling, T. E.; Mason, R. P. *J. Biol. Chem.* **1992**, *267*, 23583–23588. (e) Hoganson, C. W.; Babcock, G. T. *Biochemistry* **1992**, *31*, 11874–11880.

(3) (a) Wagner, A. F.; Frey, M.; Neugebauer, F. A.; Schäfer, W.; Knappe, J. *Proc. Natl. Acad. Sci. U.S.A.* **1992**, *89*, 996–1000. (b) Frey, M.; Rothe, M.; Wagner, A. F. V.; Knappe, J. *J. Biol. Chem.* **1994**, *269*, 12432–12437. (c) Parast, C. V.; Wong, K. K.; Lewis, S. A.; Kozarich, J. W.; Peisach, J.; Magliozzo, R. S. *Biochemistry* **1995**, *34*, 2393–2399.

(4) (a) Booker, S.; Licht, S.; Broderick, J.; Stubbe, J. *Biochemistry* **1994**, *33*, 12676–12685. (b) Norlund, P.; Eklund, H. *J. Mol. Biol.* **1993**, *232*, 123–164.

(5) Harkins, T. T.; Grissom, C. B. *Science* **1994**, *263*, 958–960.

(6) (a) Kulmacz, R. J.; Palmer, G.; Wei, C.; Tsai, A.-L. *Biochemistry* **1994**, *33*, 5428–5439. (b) Picot, D.; Loll, P. J.; Garavito, R. M. *Nature* **1994**, *367*, 243–249.

(7) Ögel, Z. B.; Brayford, D.; McPherson, M. J. *Mycol. Res.* **1994**, *98*, 474–480.

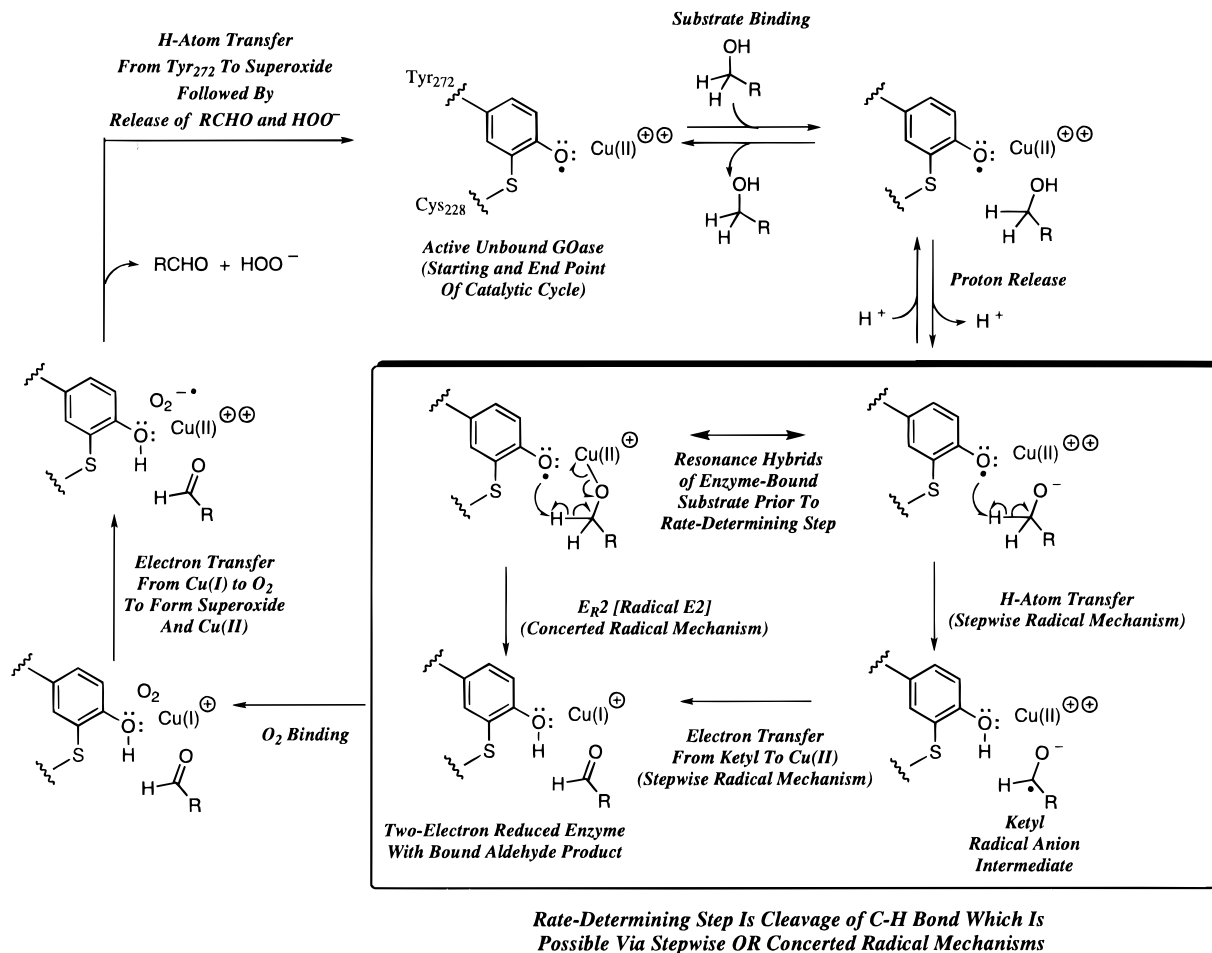
(8) (a) Kosman, D. J. in *Copper Proteins and Copper Enzymes*; Lontie, R., Ed.; CRC Press: Boca Raton, FL, 1984; Vol. 2, pp 1–26. (b) Hamilton, G. A. in *Copper Proteins. Metals Ions in Biology*; Spiro, T. G., Ed.; John Wiley & Sons: New York, 1981; Vol. 3, pp 193–218. (c) Ettinger, M. J.; Kosman, D., J. In *Copper Proteins. Metals Ions in Biology*; Spiro, T. G., Ed.; John Wiley & Sons: New York, 1981; Vol. 3, pp 219–261.

(9) (a) Hamilton, G. A. *Biochem. Biophys. Res. Commun.* **1973**, *55*, 333–340. (b) Hamilton, G. A.; Adolf, P. K.; deJersey, J.; DuBois, G. C.; Dyrkacz, G. R.; Libby, R. D. *J. Am. Chem. Soc.* **1978**, *100*, 1844–1859.

(10) (a) Driscoll, J. J.; Kosman, D. K. In *Biological and Inorganic Copper Chemistry*; Karlin, K. D., Zubieta, J., Eds.; Adenine Press: Guilderland, NY, 1986; pp 75–82. (b) Driscoll, J. J.; Kosman, D. K. *Biochemistry* **1987**, *26*, 3429–3436.

(11) Van der Meer, R.; Jongegan, J. A.; Duine, J. A. *J. Biol. Chem.* **1989**, *264*, 7792–7794.

**Scheme 1.** Two Possible Radical Mechanisms for Galactose Oxidase—Stepwise Catalysis via a Ketyl Radical Intermediate versus Concerted E2-like Oxidation of the Alcohol, Either Mechanism Using Tyrosine 272 and Copper as One-Electron Redox Centers



tallographic evidence show that this proposal is incorrect—there is no PQQ in GOase.<sup>12,13</sup>

It is now established that GOase contains two one-electron redox centers, the well-known mononuclear copper center and a tyrosine center covalently cross-linked (at the ortho position to the -OH) to a cysteine (i.e.; Tyr 272 and Cys 228 cross-link).<sup>12,13</sup> The unusual Tyr 272 is one of the equatorial ligands of the square-pyramidal copper center. GOase can exist in three distinct, stable oxidation states.<sup>14</sup> These can be assigned as highest oxidation state = Cu(II) and tyrosine radical, intermediate oxidation state = Cu(II) and tyrosine (in equilibrium with Cu(I) and tyrosine radical), and lowest oxidation state = Cu(I) and tyrosine. Spectroscopic evidence strongly indicates that a tyrosine radical is the radical center, that the tyrosine radical is directly coordinated to the copper center, and that the highest oxidation state of GOase is the catalytically active form of the enzyme.<sup>12,14</sup>

Before a structural model of GOase became available from X-ray crystallographic data, Whittaker proposed a new type of radical mechanism utilizing the tyrosine-like protein radical that he had detected based on extensive spectroscopic evidence.<sup>14</sup> Taking advantage of the structural data from X-ray crystallography<sup>13</sup> and kinetic evidence with radical-probing sub-

strates,<sup>15</sup> we proposed a more detailed mechanistic scheme.<sup>16</sup> Whittaker subsequently refined the mechanism further—we proposed that the alcohol is deprotonated by a nearby histidine acting as a base, but spectroscopic studies of anion binding to galactose oxidase lead Whittaker to propose that tyrosine 495 could act as the base.<sup>17</sup> Although there are some minor differences in the proposed mechanisms, the central feature of them all is that enzymic catalysis is proposed to proceed by a stepwise radical mechanism with a substrate derived ketyl radical as a key intermediate (Scheme 1). In the course of our ongoing studies on the mechanism of galactose oxidase using radical-probing substrates<sup>15</sup> we were led to consider the possibility of a concerted mechanism (Scheme 1). The concerted mechanism may at first appear to be unusual but it is simply a radical analog of an E2 elimination reaction, and thus might be called an  $E_{R2}$  reaction, a concerted elimination reaction with a radical starting material and a radical product. Note that both the stepwise and concerted mechanisms are consistent with mechanistic evidence from kinetic studies including (1) an ordered binding mechanism with substrate bindings and product releases occurring in the order shown and (2) cleavage of the  $\alpha$  C-H bond as the fully rate-determining step (known from the

(12) Babcock, G. T.; El-Deeb, M. K.; Sandusky, P. O.; Whittaker, M. M.; Whittaker, J. W. *J. Am. Chem. Soc.* **1992**, *114*, 3727–3734.

(13) Ito, N.; Phillips, S. E.; Stevens, C.; Ogel, Z. B.; McPherson, M. J.; Keen, J. N.; Yadav, K. D. S.; Knowles, P. F. *Nature* **1991**, *350*, 87–90.

(14) Whittaker, M. W.; Whittaker, J. W. *J. Biol. Chem.* **1988**, *263*, 6074–6080.

(15) The results of the radical-probing substrate studies will be published elsewhere.

(16) Branchaud, B. P.; Montague-Smith, M. P.; Kosman, D. J.; McLaren, F. R. *J. Am. Chem. Soc.* **1993**, *115*, 798–800.

(17) Whittaker, M. M.; Whittaker, J. W. *Biophys. J.* **1993**, *64*, 762–772.

nearly full primary deuterium isotope effect when the  $\alpha$  position is substituted with deuterium).<sup>18</sup>

We were interested in whether the topology of the active site is consistent with the proposed radical mechanisms in Scheme 1. Since cleavage of the  $\alpha$  C–H bond is fully rate determining, it is possible to compare experimental results of known substrate specificities with molecular modeling results of proposed mechanisms for C–H bond cleavage. Such molecular modeling studies might allow one to rule out, or at least disfavor, one of the proposed mechanisms. For example, the concerted E2-like mechanism might seem less plausible if the enzyme–substrate fit was inconsistent with the stringent stereoelectronic orbital alignment (orbital overlap) requirements of a concerted E2-like mechanism. At the very least, molecular modeling studies could indicate that both mechanisms were plausible and worthy of continued consideration.

Previously a computer graphic study of manual docking of substrates into the active site structure of GOase was used to gain insight into possible important enzyme–substrate interactions.<sup>19</sup> The chair conformation of  $\beta$ -D-galactose, a good substrate of GOase, was shown to have a high degree of shape and electrostatic complementarity to the active site. Manual docking of D-glucose in the active site indicated that unfavorable steric clashes and loss of hydrogen bonding interactions (compared to D-galactose) could explain why D-glucose is not a substrate. The manual docking studies examined enzyme–substrate interactions, not enzyme–transition state interactions. They were also qualitative in that no energy calculations were performed. Good arguments can be made that such studies are often sufficient to understand the main points of enzyme–substrate interactions but they are probably not sufficient to examine detailed mechanistic questions.

In this paper we use molecular mechanics calculations of binding of radical hydrogen atom transfer transition structures in the GOase active site to examine whether radical mechanisms are consistent with known substrate specificities of GOase. Although GOase will process a wide variety of primary alcohol substrates, it is highly selective in its processing of hexopyranose substrates. There are two especially significant examples of hexopyranose substrate specificity which can be used to examine possible radical mechanisms. (1) Turnover of D-galactose is stereospecific for abstraction of the *pro-S* hydrogen.<sup>18</sup> *Is the pro-S stereospecificity for D-galactose consistent with either or both of the radical mechanisms shown in Scheme 1?* (2) Although D-galactose is an excellent substrate ( $k_{\text{cat}}$  as high as  $700 \text{ s}^{-1}$  at pH 7.0 and 25 °C for a high-quality preparation of enzyme), its C-4 epimer D-glucose is not a substrate<sup>20</sup> and will not bind to the enzyme at concentrations as high as 1 M.<sup>21</sup> *Is the high selectivity for D-galactose as an excellent substrate and against its C-4 epimer D-glucose consistent with either or both of the radical mechanisms shown in Scheme 1?*

## Materials and Methods

**Molecular Mechanics Computations.** The inter- and intramolecular interactions were modeled by the DREIDING-II force field<sup>22</sup> (Biograf version 3.21 modeling software by Molecular Simulations, Inc.) on a Silicon Graphics Indigo workstation. This force field uses a restricted set of parameters consisting of general force constants and

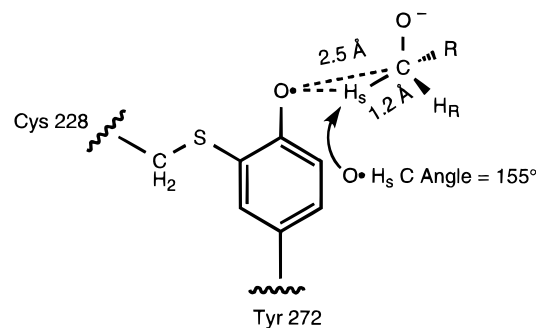


**Figure 1.** Fixed H-atom transfer transition state geometry used for molecular mechanics calculations.

geometry parameters based on simple hybridization considerations. There is only one force constant each for bonds, angles, and inversions, and only six different values for torsional barriers. This approach was shown to lead to accurate geometries and reasonably accurate energies for various organic systems.<sup>22</sup> For the hexopyranose ligands, an all-atom representation was employed. For the protein, the united-atom or extended-atom approximation was used,<sup>23</sup> with explicit representation of hydrogens only when attached to heteroatoms. The energetics of bond stretching, angle bending, dihedral angle torsions, van der Waals, and hydrogen bonding interactions were modeled using standard parameters of the program unless explicitly stated otherwise. In all cases, Coulombic calculations were excluded due to the difficulty in modeling the electrostatics of the copper ion in its coordination sphere, so that the van der Waals repulsion of atoms involved in hydrogen bonding is not offset by an electrostatic term. The explicit CHARMM-like hydrogen-bonding potential itself underestimates the overall strength of a hydrogen bond, so that hydrogen bonding is a relatively minor factor during minimization. The minimum is largely determined by the bonded terms of the ligand itself and shape complementarity to the protein active site.

**Transition State Geometry for H-Atom Transfer from Alcohol  $\alpha$  C–H to Tyrosine 272.** A fixed nonlinear geometry of the H-atom transfer was used with the  $\text{C}\cdots\text{H}\cdots\text{O}$  bond angle at  $155^\circ$ , the  $\text{C}\cdots\text{O}$  distance at 2.5 Å, and the C–H distance at 1.2 Å (Figure 1). This results in a  $\text{O}\cdots\text{H}$  separation of 1.36 Å. This particular geometry was taken directly from transition state models of intramolecular H-atom abstractions by alkoxy radicals, which in turn were based on detailed ab initio calculations carried out for the  $\cdot\text{OH} + \text{CH}_4$  reaction.<sup>24</sup> A justification of this choice of transition state geometry is given in the Results and Discussion section.

**Choice of Fixed Distance from Copper to the Oxygen of the Alcohol Substrate.** The distance of O to copper was constrained to 2.3 Å, equal to the oxygen–copper distance for acetate in the crystal structure. The other three equatorial coordination distances are 1.9, 2.1, and 2.2 Å for  $\text{O}^\ominus$  of Tyr 272,  $\text{N}^\ominus$  of His496, and  $\text{N}^\ominus$  of His581 respectively, close to the 2.3 Å constraint.<sup>19</sup>

**Protein Coordinates.** GOase coordinates were kindly provided to us by Simon Phillips of the University of Leeds prior to public release, and are now deposited in the Brookhaven National Laboratory Protein Data Bank.<sup>25</sup> Coordinates are available for the native structure at pH 4.5, which has been refined to 1.7 Å resolution, the native structure at pH 7.0, which has been refined to 1.9 Å resolution, and the apoenzyme with the copper removed, which has been refined to 2.2 Å.<sup>19</sup> The three structures are essentially identical, and the coordinates for the native structure at pH 4.5, the highest-resolution structure, are used here. Hydrogens were added to all heteroatoms, using the united atom approximation.<sup>23</sup> Water and acetate molecules present in the structural models derived from X-ray crystallographic studies were excluded from all calculations.

The protein itself was held completely rigid during all mechanics calculations, since it was assumed that the enzyme does not undergo a

(18) Maradufu, A.; Cree, G. M.; Perlin, A. S. *Can. J. Chem.* **1971**, *49*, 3429–3437.

(19) Ito, N.; Phillips, S. E. V.; Yadav, K. D. S.; Knowles, P. F. *J. Mol. Biol.* **1994**, *238*, 794–814.

(20) Amaral, D.; Kelly-Falcoz, F.; Horecker, B. L. *Methods Enzymol.* **1966**, *9*, 87–92.

(21) Wachter, Rebekka, unpublished observation.

(22) Mayo, S. L.; Olafson, B. D.; Goddard III, W. A. *J. Phys. Chem.* **1990**, *94*, 8897–8909.

(23) McCammon, A.; Harvey, S. C. *Dynamics of Proteins and Nucleic Acids*; Cambridge University Press: Cambridge, 1987; p 41.

(24) Dorigo, A. E.; Houk, K. N. *J. Org. Chem.* **1987**, *53*, 1650–1664.

(25) Bernstein, F. C.; Koetzle, T. F.; Williams, G. J. B.; Meyer, E. F., Jr.; Brice, M. D.; Rodgers, J. R.; Kennard, O.; Shimanouchi, T.; Tasumi, M. *J. Mol. Biol.* **1977**, *112*, 535–542.

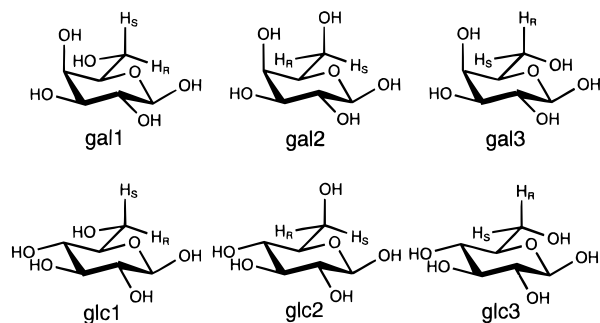


**Figure 2.** Galactose and glucose conformations used as starting structures for molecular mechanics minimization of active-site-bound transition states.

conformational change to bind galactose. This appeared reasonable since no structural rearrangements were observed crystallographically when changing pH or removing copper,<sup>19</sup> and since the protein was reported to be active in 6 M urea, a typical protein denaturant.<sup>26</sup> The active site, a shallow indentation of the protein surface with the copper bound at the bottom of the groove, is rich in aromatic residues, with a large number of aromatic–aromatic stacking and edge-to-face interactions.<sup>27</sup> This factor together with the covalent cross-link between Tyr 272 and Cys 228 is thought to render the active site rather rigid. Though some “breathing” of the active site is likely to occur, these kinds of motions cannot be included in the calculations performed here.

**Modeling Procedure.**  $\beta$ -D-galactose and  $\beta$ -D-glucose were drawn in vacuo in the chair conformation. Both hexopyranoses were minimized in all three staggered rotational conformations around the C5–C6 bond, resulting in a total of six structures, named gal1, gal2, and gal3 for the galactose rotamers, and glc1, glc2, and glc3 for the glucose rotamers (Figure 2). Gal1, gal2, and gal3 had essentially the same bond, angle, torsional, and van der Waals energies in the DREIDING force field, though it has been reported that the most favorable conformation is gal1, with a *trans* torsion angle around O5–C5–C6–O6 (Figure 2).<sup>18</sup> In the case of glucose, glc2 and glc3 had essentially the same energies as the galactose conformers, whereas for glc1 slightly higher bond, angle, torsional, and van der Waals energies were calculated. Glc1 was also the only hexopyranose structure in which an intramolecular H-bond was recognized by the program, lowering the total energy below that of the other galactose and glucose structures.

Each conformer was manually docked into the active site so that O6 was positioned at the “empty” equatorial copper coordination site, occupied by solvent-derived acetate in the crystal structure. This was accomplished by overlaying O6 onto the acetate oxygen. The hexopyranose was then manually rotated as a rigid body so that either the *pro-S* or the *pro-R* hydrogen of C6 pointed at the oxygen of Tyr 272. The intention was to position the ligand close to a binding mode that would allow reaction to occur at only one of the two hydrogens of C6. Manual docking was carried out only to find a conformation consistent with the chemical reaction under consideration, with close proximity of the hydrogen in question to the oxy radical. The overall fit of the substrate into the active site was not considered at this point.

Each bound structure was then energy-minimized, allowing the ligand to be flexible while maintaining a series of constraints forcing the reacting atoms into the desired transition state geometry. The positions of the reacting atoms were then fixed in place with no energetic terms associated with them: (1) a fixed nonlinear geometry of the H-atom transfer was used with the hexopyranose C6 to O<sup>Tyr</sup> 272 distance at 2.50 Å, the C6···H···O<sup>Tyr</sup> 272 bond angle at 155°, and the C6–H distance at 1.2 Å, and (2) the distance of O6 to copper was fixed at 2.3 Å. The structures were then reminimized to give the final geometry used for analysis.

**Analysis.** The resulting structures were named according to the hydrogen transferred, e.g., gal1S denoting the gal1 rotamer modeled into the active site with the *pro-S* hydrogen in the transition state. For

each structure, the difference in bond, angle, torsional and van der Waals energies between the free and bound ligand was calculated (Table 1). To analyze potential hydrogen bonding, a statistical analysis of stereochemical hydrogen bonding preferences in proteins was consulted.<sup>28</sup> Average hydrogen bonding distances for Arg, Trp, and Tyr, the polar amino acids lining the active site of GOase, were reported to be 3.0 (0.2), 3.0 (0.2), and 2.9 (0.3) Å within protein structures (standard deviations in parentheses). The coordinate error in the GOase structure was estimated to be 0.16 Å,<sup>19</sup> so that potential hydrogen bonding interactions were selected based on a cutoff distance of 3.4 Å for the non-hydrogen atom separations.

In the case of Arg and Trp as hydrogen bond donors, an N–H···O<sub>acceptor</sub> angle between 140° and 180° was accepted since the average angle of this type in proteins was reported to be 155°, with 90% occurring between 140° and 180°. In the case of either tyrosine or sugar hydroxyls as donors, the C–O···O<sub>acceptor</sub> angle was examined and fell within one standard deviation of the published statistics in all modeled structures. The average angle for tyrosine was reported to be 119°(14°).<sup>28</sup> The sugar hydroxyls were assumed to be subject to the same statistics as serines and threonines, where the average angle was reported to be 116°(18°). Based on these distance and angle criteria, the number of hydrogen bonds for each tested conformation was listed (Table 1).

Close van der Waals contacts or steric clashes of sugar hydroxyls with a hydrophobic surface were tabulated if the hydroxyl hydrogen bonding potential appeared to be unsatisfied by the protein (Table 1). To this end, a cutoff of 4 Å for the non-hydrogen atom distance was chosen.<sup>29,30</sup> The position of the O6 in relation to the other equatorial ligands was analyzed by tabulating the angle between the plane of N<sup>His</sup> 496, N<sup>His</sup> 581, and O<sup>Tyr</sup> 272 and the plane of N<sup>His</sup> 496, O<sup>Tyr</sup> 272, and O6 of the hexopyranose ligand (Table 1).

## Results and Discussion

**Choice of Transition State Geometry.** Calculations have been done on the transition state geometries of several H-atom abstractions by alkoxy radicals, all leading to similar geometries regardless of how exothermic or endothermic a particular reaction is. The highly exothermic reaction of HO• with CH<sub>4</sub> ( $\Delta H = -14$  kcal/mol, based on standard bond energies) has been calculated to have the C···H···O bond angle at 171°, the C···O distance at 2.5 Å, and the C–H distance at 1.2–1.3 Å.<sup>24</sup> In contrast, the endothermic reaction of *p*-nitrosophenoxy radical with ethane ( $\Delta H =$  at least +12–13 kcal/mol, based on standard bond energies) has been calculated to have the C···H···O bond angle at 169°, the C···O distance at 2.5 Å, and the C–H distance at 1.3 Å.<sup>31</sup> The somewhat exothermic intramolecular reaction of an alkoxy radical with primary or secondary C–H ( $\Delta H = -4$ –8 kcal/mol, based on standard bond energies) has been calculated to have the C···H···O bond angle at 155°, the C···O distance at 2.5 Å, and the C–H distance at 1.2 Å.<sup>24</sup> This last geometry was used in the studies reported here because the reaction of the tyrosine radical in galactose oxidase with a copper-coordinated alkoxide should be only slightly endothermic, and possibly slightly exothermic, due to the weakening of the C–H bond in the alkoxide due to the oxyanion effect.<sup>32</sup>

The main difference in these different calculated transition state geometries is in the C···H···O bond angle. In all structures examined, we found that molecular mechanics minimizations using a C···H···O bond angle of 155° provided a reasonable O6···C6···H angle (angle at alcohol undergoing oxidation) of

(28) Ippolito, J. A.; Alexander, R. S.; Christianson, D. W. *J. Mol. Biol.* **1990**, *215*, 457–471.

(29) Zou, J.; Flocco, M. M.; Mowbray, S. L. *J. Mol. Biol.* **1993**, *233*, 739–752.

(30) Spurlino, J. C.; Lu, G.-Y.; Quiocho, F. A. *J. Biol. Chem.* **1991**, *266*, 5202–5219.

(31) Korzekwa, K. R.; Jones, J. P.; Gillette, J. R. *J. Am. Chem. Soc.* **1990**, *112*, 7049–7046.

(32) Steigerwald, M. L.; Goddard, W. A., III; Evans, D. A. *J. Am. Chem. Soc.* **1979**, *101*, 1994–1997.

(26) Kosman, D. J.; Ettinger, M. J.; Weiner, R. E.; Massaro, E. J. *Arch. Biochem. Biophys.* **1974**, *165*, 456–467.

(27) For a review on weakly polar interactions in proteins, see Burley, S. K.; Petsko, G. A. *Adv. Protein Chem.* **1988**, *39*, 125–189.

**Table 1.** Energetic Analysis of a Series of Test Structures Obtained by Modeling the Transition State for Reaction of Galactose Oxidase with Galactose and Glucose

| structure <sup>a</sup> | $\Delta$ bond <sup>b</sup> | $\Delta$ angle <sup>b</sup> | $\Delta$ torsion <sup>b</sup> | $\Delta$ vdW <sup>b</sup> | no. of H-bonds <sup>c</sup> | philicphobic <sup>d</sup> | amino acids contacted <sup>d</sup> | equatorial plane angle <sup>e</sup> (deg) |
|------------------------|----------------------------|-----------------------------|-------------------------------|---------------------------|-----------------------------|---------------------------|------------------------------------|---|
| gal1S                  | +0.075                     | +1.14                       | +0.12                         | -11.2                     | 5                           | none                      |                                    | 7.7                                       |
| gal1R                  | +0.135                     | +4.98                       | +1.19                         | -2.01                     | 1                           | none                      |                                    | 6.2                                       |
| gal2S                  | -0.382                     | +0.954                      | +1.294                        | -6.36                     | 2                           | O4                        | Phe464, Phe194                     | 11.5                                      |
|                        |                            |                             |                               |                           |                             | O5                        | Tyr495                             |   |
| gal2R                  | +0.406                     | +5.12                       | +3.46                         | +1.36                     | 0                           | O3                        | Phe194                             | 11.5                                      |
|                        |                            |                             |                               |                           |                             | O4                        | Phe194, Phe464                     |   |
| gal3S                  | +0.499                     | +1.58                       | +1.82                         | -5.78                     | 2                           | O4                        | Phe194                             | 14.5                                      |
|                        |                            |                             |                               |                           |                             | O5                        | Phe464                             |   |
| gal3R                  | -0.003                     | +2.81                       | +0.30                         | -7.00                     | 2                           | none                      |                                    | 20.3                                      |
| glc1S                  | -0.38                      | +1.92                       | -0.65                         | -13.05                    | 2                           | O4                        | Tyr495, Phe464                     | 1.8                                       |
| glc1R                  | +0.31                      | +2.70                       | +1.81                         | +5.51                     | 3                           | O3                        | Phe464                             | 0.25                                      |
|                        |                            |                             |                               |                           |                             | O4                        | Phe464, Phe194                     |   |
| glc2S                  | +0.51                      | +2.05                       | +1.17                         | -7.45                     | 2                           | O4                        | Tyr495, Phe464                     | 0.65                                      |
| glc2R                  | +0.32                      | +5.40                       | +1.39                         | +3.06                     | 0                           | O3                        | Phe194                             | 12.4                                      |
|                        |                            |                             |                               |                           |                             | O4                        | Phe194, Trp290                     |   |
| glc3S                  | +0.57                      | +3.29                       | +2.15                         | -2.16                     | 2                           | O4                        | Phe464                             | 5.1                                       |
| glc3R                  | +1.66                      | +8.14                       | +2.24                         | +6.94                     | 2                           | O5                        | Phe464, Phe194                     | 1.9                                       |
| gal1S-binding          | +0.091                     | +1.64                       | +0.27                         | -12.22                    | 7                           | none                      |                                    | 2.1                                       |

<sup>a</sup> gal denotes galactose, glc denotes glucose, the numeral denotes the particular hexose rotamer used in the model (see Figure 2), S or R denotes the *pro-S* or *pro-R* C6 hydrogen positioned to react; all represent transition state models except gal1S-binding, which represents a model of the Michaelis complex. <sup>b</sup> Calculated change in bond length, bond angle, torsional, and van der Waals energy from free to bound ligand. <sup>c</sup> Potential hydrogen bonds between sugar hydroxyls and protein functional groups predicted based on statistical geometric preference (see text). <sup>d</sup> van der Waals contacts (<4 Å between non-hydrogen atoms) of non-hydrogen bonded sugar hydroxyls with a hydrophobic surface consisting of the specified amino acids. <sup>e</sup> Angle between the equatorial coordination plane defined by the three amino acid ligand atoms and the plane defined by the sugar O6 and two of the amino acid ligand atoms (see text).

105° whereas the use of a C···H···O bond angle of 169° provided an unreasonable O6···C6···H angle of 79° to 82° and the use of a C···H···O bond angle of 180° provided an unreasonable O6···C6···H angle of 73° to 76°. It may be an overinterpretation of the results but it is interesting to imagine that the galactose oxidase active site might be optimal for radical catalysis and that the best fit of a transition state geometry in the active site (C···H···O bond angle of 155°) provides some insight into the best transition state geometry for H-atom transfer (i.e., the best transition state model from molecular mechanics studies of the enzyme substrate complex is similar to the transition state model for intramolecular hydrogen atom transfer).

**Hexose Substrates Used in This Study,  $\beta$ -D-Galactose and  $\beta$ -D-Glucose.** Our test compounds consisted of two hexose:  $\beta$ -D-galactose, a good substrate of the enzyme, reported to be stereospecific toward the *pro-S* hydrogen,<sup>18</sup> and  $\beta$ -D-glucose, which is not turned over by the enzyme at all.<sup>20</sup> The result that glucose is not a substrate was so surprising that we needed to confirm it ourselves. We also tested whether glucose competes with galactose for binding to the active site by assaying galactose turnover in the presence of increasing concentrations of glucose. Galactose turnover is not decreased in the presence of glucose at concentrations up to 1 M.<sup>21</sup> We conclude that glucose is not only not oxidized by the enzyme, it also is not a competitive inhibitor, and so does not even bind to the active site. The three low-energy rotational conformers of  $\beta$ -D-galactose and the three low-energy conformers of  $\beta$ -D-glucose (Figure 2) were aligned in the active site each in two orientations, so that either the *pro-S* or the *pro-R* hydrogen was poised to react. All 12 conformations were then energy-minimized while keeping the reacting atoms in the proposed transition state geometry, as shown in Figure 1. The resulting structures were named according to the hydrogen transferred, e.g., gal1S denoting the gal1 rotamer modeled into the active site with the *pro-S* hydrogen in the transition state. The structures were then analyzed to find the most favorable

conformation by tabulating the energetic differences between the bound and free state of the ligand for each structure (Table 1).

**Molecular Modeling of Radical Carbon–Hydrogen Bond Cleavage as the Rate-Determining Step for GOase Is Consistent with either a Stepwise or a Concerted Mechanism.** The energy-minimized structure for a radical C–H cleavage of the *pro-S* C–H bond of galactose is best represented by the gal1S structure in Table 1 (for a detailed discussion of all test structures, see below). A three-dimensional representation of gal1S (Figure 3) shows clearly that this structure is consistent with either a stepwise or a concerted mechanism. This might not seem that surprising since so many constraints were imposed on the transition state geometry. However, these constraints seem fully justified for either a stepwise or a concerted mechanism. The fixed nonlinear geometry for H-atom transfer would be expected to be essentially the same for either stepwise or concerted mechanisms—i.e., there is only one proper way to line up the bonds for efficient bond-making and bond-breaking in either mechanism. Likewise, the fixed O6 to copper distance of 2.3 Å would be reasonable for either mechanism since O6 should be directly in the coordination sphere of copper for either mechanism.

The one striking feature of the structure in Figure 3 that might favor one mechanism over the other is the almost perfect orbital alignment for the concerted E2-like radical mechanism. In the transition state in Figure 3 a pseudo-five-membered ring is formed from the copper, O6 of D-galactose, C6 of D-galactose, the *pro-S* H on C6, and the phenoxy O of Tyr 272. Remarkably, these five atoms are essentially coplanar with dihedral angles near 0°, optimal for a concerted syn elimination type of mechanism.

Other structural features indicate that the active site of galactose oxidase appears to be highly evolved for catalysis of a radical mechanism, either stepwise or concerted. The incipient O–H bond between the tyrosine O and the *pro-S* H is aligned to have nearly optimal orbital overlap with the  $\pi$  electron system in the aromatic ring of Tyr 272 (i.e., it is perpendicular to the

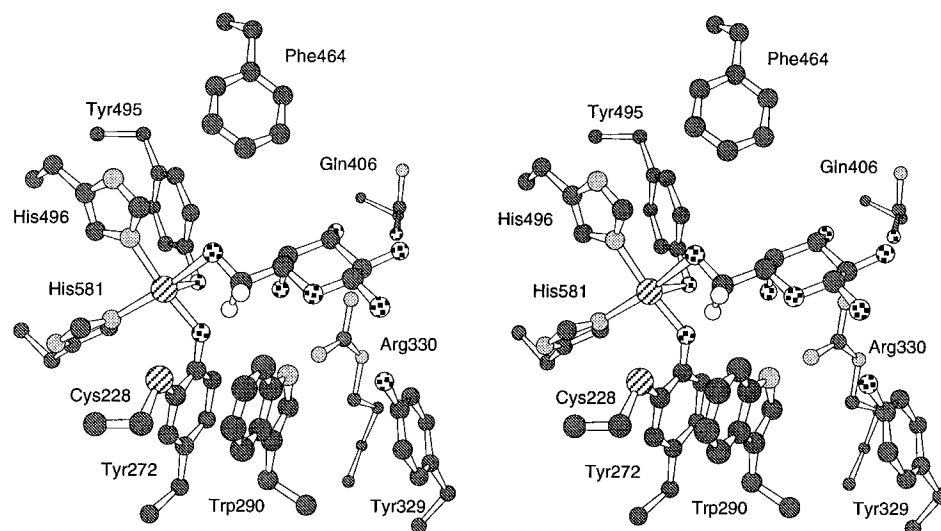


**Figure 3.** Stereoview (direct view) of a model of the transition state for abstraction of the *pro-S* hydrogen of galactose by galactose oxidase.

aromatic ring in Tyr 272 and thus lined up with a dihedral angle near  $0^\circ$  for overlap with the  $\pi$  system). The sulfur of Cys 228 should also be able to participate in the  $\pi$  delocalization. The delocalization of electron density in the transition state should provide additional stabilization to facilitate either a concerted or stepwise reaction. Finally, the stacking of the electron-rich indole ring of tryptophan 290 over the electron-deficient tyrosine radical on Tyr 272 may provide some  $\pi$ -stacking and/or charge-transfer stabilization.

**Molecular Modeling of Radical Carbon–Hydrogen Bond Cleavage (Stepwise or Concerted Mechanisms) as the Rate-Determining Step for GOase Explains the Known Stereoselective Cleavage of the *pro-S* C–H Bond at C6 in Galactose.** The most striking difference between the gal1S transition state structure and all others is the number of hydrogen bonds. When using a cutoff of  $3.4 \text{ \AA}$ , five hydrogen bonds are predicted to occur in this conformation, and when using a cutoff of  $3.5 \text{ \AA}$ , seven H-bonds are predicted. All other galactose conformations give between 0 and 2 hydrogen bonds, indicating preferred energetics in the gal1S conformation (Table 1). The change in substrate bond energy from free to bound ligand does not vary significantly. The change in angle energy is positive in all cases, but smallest in the gal1S and gal2S conformations. Disfavorable torsions are lowest in gal1S among the galactose structures. Gal1S, also having the most favorable van der Waals energy among the galactose structures, apparently fits into the active site quite well.

The last column (Table 1) lists the angle between the planes formed by two sets of equatorial ligands, one of them including the hexopyranose O6, and so is a measure of equatorial planarity in the presence of ligand (see Materials and Methods). This angle is  $6.6^\circ$  for the acetate ligand bound in the crystal structure, and  $7.7^\circ$  for the gal1S structure. The position of the acetate oxygen is only  $0.3 \text{ \AA}$  away from the proposed position of galactose O6 in the transition state of gal1S. In comparison, all other galactose structures give considerably larger angles, resulting in distortion of equatorial coordination symmetry that is not consistent with the crystal structure.

In summary, a qualitative analysis of binding energetics predicts that D-galactose binds as the gal1 rotamer, as previously proposed by Ito et al.<sup>19</sup> Favorable interactions, in particular hydrogen bonding and van der Waals contacts, are maximized by positioning the *pro-S* hydrogen to react with the protein radical. Transition state modeling based on a radical mechanism gives a very satisfying explanation for the observed stereospecificity of the enzyme.

**Molecular Modeling of Radical Carbon–Hydrogen Bond Cleavage (Stepwise or Concerted Mechanisms) as the Rate-Determining Step for GOase Explains the Fact that Galactose Is an Excellent Substrate whereas Glucose Is Not a Substrate and Does Not Even Bind to the Active Site.** Little strain is introduced into the ligand structure in both the gal1S and glc1S structures. In both cases, the van der Waals energy change upon binding, a measure of shape complementarity, is significantly more favorable than in the others (Table 1). It appears that gal1S and glc1S fit into the active site quite well. The difference in number of hydrogen bonds is significant (5 vs 2), but this fact alone is not sufficient to give a satisfactory explanation for the observed inability of glucose to bind. In the most favorable glucose structure, glc1S, a steric clash between O4 and a ring carbon of Tyr 495 is observed (Table 1). This unfavorable steric interaction was predicted previously in a qualitative manner when simple *ground state* binding was modeled by manual docking techniques.<sup>19</sup> It is thought to contribute toward discrimination against glucose binding.

Analysis of close hydrophilic–hydrophobic contacts leads to a rather striking observation (Table 1). The only conformations without such electrostatically unfavorable contacts are gal1S, gal1R, and gal3R. All others, including all glucose structures, have sugar hydroxyl groups O3, O4, or O5 in close van der Waals contact with a hydrophobic surface consisting of Phe 464, Phe 194, Trp 290, or Tyr 495. These hydroxyls have no potential protein hydrogen-bonding partners in their vicinity, and O4 and O5 are sequestered well away from bulk solvent after binding.

We propose that the three glcS conformations, though they show a favorable van der Waals energy change, do not represent viable structures due to close contact between the hydrophilic O4 hydroxyl group and a hydrophobic surface consisting of the axial copper ligand Tyr 495, and Phe 464. This appears to be a more general strategy used by carbohydrate-binding proteins to achieve a high degree of specificity toward anomer and epimer recognition.<sup>30,33</sup> From an energetic point of view, it is entirely reasonable. For example, when serines and threonines were introduced into the hydrophobic core of T4 lysozyme, it was found that the protein structure adapted in all cases to avoid the presence of unsatisfied hydrogen bonding potential.<sup>34</sup> This is consistent with the view that buried polar groups that lack a

(33) Vyas, N. K. *Curr. Opin. Struct. Biol.* **1991**, *1*, 732–740.

(34) Blaber, M.; Lindstrom, J. D.; Gassner, N.; Xu, J.; Heinz, D. W.; Matthews, B. W. *Biochemistry* **1993**, *32*, 11363–11373.

hydrogen-bonding partner are very destabilizing to protein integrity.

In summary, D-glucose is predicted not to bind due to a severe hydrophilic-hydrophobic clash, and also some steric interference. This prediction is born out by experiment, and so lends further support to the proposed transition state geometry.

**Analysis of Predicted Transition State Protein–Ligand Interactions of Gal1S.** Setting the cutoff distance for hydrogen bonding at 3.4 Å results in the prediction of 5 hydrogen bonds (Figure 5). Galactose O1 is a hydrogen bond donor to the O<sup>γ</sup> of Tyr 329, O3 is a hydrogen bond acceptor to the N<sup>η1</sup> of Arg 330, O4 is both acceptor to N<sup>η2</sup> of Arg 330 and donor to O<sup>γ</sup> of Tyr 495, and O5 is acceptor to N<sup>ε</sup> of Trp 290. If the cutoff distance is set to 3.5 Å, O3 is predicted to also be involved in a donor interaction with the O<sup>ε</sup> of Gln 406, and O4 to be involved in an acceptor interactions, with N<sup>η1</sup> of Arg 330. If this was the case, the complete hydrogen-bonding potential of O4, i.e., two acceptor and one donor interaction, would be realized, resulting in cooperative hydrogen bonding.<sup>33</sup> These interactions would be lost in the case of glucose, giving special importance to the axial position of this hydroxyl in galactose. With the higher cutoff, the N<sup>η1</sup> of Arg 330 would be a bifurcated H-bond donor to both O3 and O4. In either case, Arg 330 would be a bidentate hydrogen bond donor to both O3 and O4.

Overall, the hydrogen-bonding scheme is completely consistent with other carbohydrate-binding proteins, where an overwhelming preference of a sugar hydroxyl to accept a hydrogen bond from NH groups and to donate a hydrogen bond to oxygen atoms has been noted.<sup>33</sup> A bidentate interaction with adjacent axial and equatorial sugar hydroxyls is also common. The scheme is reasonable since the only hydroxyl without a protein hydrogen-bonding partner is O2, which is exposed to bulk solvent at the protein surface. O1 is close to the protein surface as well, so that the sugar may bind in an oligomeric form without interfering with the above described interactions. Oligosaccharides have previously been found to increase the catalytic rate 2- to 6-fold as compared to galactose turnover.<sup>20</sup>

When the galactose electrostatic van der Waals surface is modeled (not shown), it is obvious that the B-face is considerably more hydrophobic than the A-face. The A-face of a sugar is defined as that for which the numbering of the carbon atoms is clockwise, and the B-face counterclockwise.<sup>30</sup> A much larger area of apolar C–H groups protrude from the B-face than from the A-face of galactose. The A-face contains the axial O4. The stacking of aromatic residues against the faces of sugars has been found in all but one of the protein–carbohydrate complex structures determined so far.<sup>30,33</sup> In the gal1S conformation, the B-face is involved in close contact of sugar carbons C3 and C4 with Phe 464, with a C···C distance of 4.2 Å in both cases. The A-face is involved in close approach of sugar C5 with one of the carbons of Trp 290, with a C···C distance of 4.5 Å. The distances cited are somewhat larger than the 4-Å cutoff employed for similar analyses of other carbohydrate-binding proteins.<sup>29,30</sup> This is reasonable since some types of interactions typically found in proteins involve atoms separated by 4.5 Å, well outside normal van der Waals contacts.<sup>35</sup> Also, a completely rigid active site has been assumed here. Small movements of protein side chains upon binding are conceivable.

**The Transition State Structure Exhibits Increased Stabilization over the Proposed Michaelis Complex.** Simple binding without transition state constraints was also modeled for binding of β-D-galactose in the gal1S conformation (Figure 4). Working “backwards”, the transition state geometry was “loosened” by relaxing all mechanistic constraints. The only

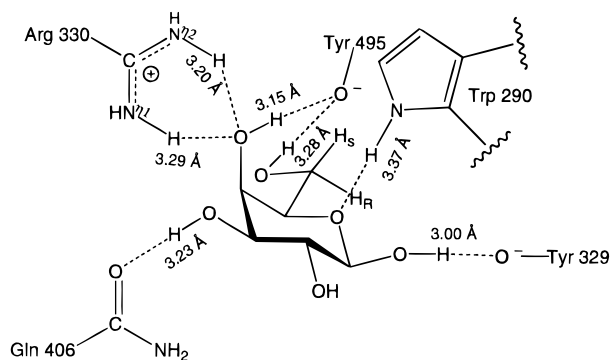


**Figure 4.** Schematic representation of key *ground state* GOase–galactose interactions.

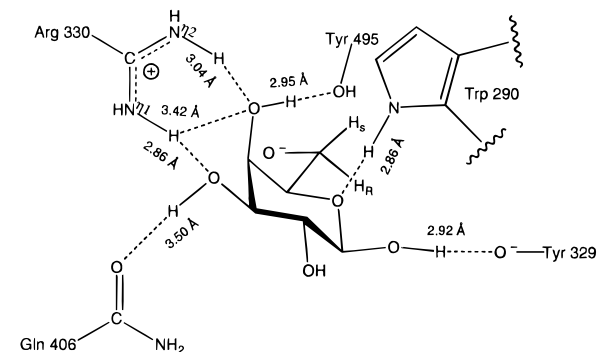


**Figure 5.** Schematic representation of key *transition state* GOase–galactose interactions.

constraint kept in place was the Cu···O6 distance of 2.3 Å to model coordination to copper during binding, with the entire sugar monomer now allowed to be flexible during minimization.

The following changes are observed when comparing the model for simple ground state binding (Figure 4) with the transition state model (Figure 5). (1) A hydrogen bond between O3 and O<sup>ε</sup> of Gln 406 in the binding model would be decreased in strength in the transition state model. (2) A hydrogen bond between O3 and N<sup>η1</sup> of Arg 330 would be gained in the transition state based on an improved angle. (3) In the binding model both N<sup>η1</sup> and N<sup>η2</sup> of Arg 330 donate a hydrogen bond equally to O4, whereas in the transition state the N<sup>η1</sup> interaction with O4 is weakened and the N<sup>η2</sup> interaction is much improved due to closer approach. (4) The O5 to N<sup>ε</sup> Trp 290 hydrogen bond is considerably shorter, and so much stronger in the transition state. (5) The hydrogen bond between O4 and O<sup>γ</sup> of Tyr 495 is also considerably strengthened in the transition state due to much closer approach. A three-dimensional representation of these interactions is shown in the stereoview in Figure 3.

We speculate that initial binding is based on sugar interactions with both polar and aromatic residues, and that these interactions are improved in the transition state, mainly by the action of Arg 330, Trp 290, and Tyr 495, stabilizing the transition state by optimizing hydrogen-bonding interactions. In this scenario, Arg 330 is initially involved in a weaker bidentate interaction with O4, then forms a strong hydrogen bond to O4 with mostly one of the nitrogens in the transition state, while involving the other nitrogen in a separate interaction. Arg 330, in conjunction with Tyr 495 and Trp 290, is thought to facilitate catalysis by pulling the substrate further toward the transition state, paying the energetic cost of close proximity of reacting centers in the transition state by improving hydrogen-bonding interactions. It is interesting to note that all three amino acids proposed to be intimately involved in the formation of the transition state are also participating in stacking and edge-to-face interactions with

other aromatics. Trp 290 is stacked onto Tyr 272, the site of the protein radical, and also forms an aromatic–aromatic edge-to-face interaction with Tyr 329 with an interplanar angle of  $26^\circ$ , close to the  $20^\circ$  optimum described.<sup>27</sup> Tyr 495 forms an edge-to-face interaction with Phe 464 at an interplanar angle of  $82^\circ$ , close to the  $90^\circ$  optimum described.<sup>27</sup> Arg 330 is stacked onto Tyr 405, based on the N $^\epsilon$  of Arg 330 being centered in the middle of the aromatic ring of Tyr 405, with N $^\epsilon$  distances to the tyrosine ring carbons ranging from 3.6 to 4.9 Å. This type of interaction is often found in locations critical to the function of proteins, and is thought to serve to orient the arginine side chain without interfering with its ability to form hydrogen bonds elsewhere.<sup>35</sup> In summary, the above aromatic–aromatic interactions are thought to function in keeping all groups essential for catalysis in a rigid, properly oriented conformation.

### Conclusions

In summary, transition state modeling of radical carbon–hydrogen bond cleavage (stepwise or concerted mechanisms) as the rate-determining step in hexopyranose turnover by GOase

gave results consistent with experimental observations of stereospecificity toward the *pro-S* hydrogen of D-galactose and strict discrimination against D-glucose as a substrate or ligand. The modeling studies cannot discriminate between stepwise or concerted mechanisms although stereoelectronic considerations of orbital overlap make a concerted mechanism especially attractive. Regardless of whether a stepwise or a concerted mechanism is operating it is clear that the active site of galactose oxidase is highly evolved to catalyze the radical oxidation of alcohols to aldehydes. Significant differences are found in comparisons of the transition state model versus the ground state model for galactose, suggesting again that galactose oxidase is designed to bind radical transition states and perform radical enzyme catalysis.

**Acknowledgment.** We are grateful to the National Science Foundation (Grant MCB-9311514) and the National Institutes of Health (Graduate Training in Molecular Biology and Biophysics 2T32GM07759) for support of this research.

JA9519896